Communication

THE JOURNAL OF BIOLOGICAL CHEMISTRY
Vol. 271, No. 21, Issue of May 24, pp. 12141–12144, 1996
Printed in U.S.A.

Enzyme-DNA Interactions Required for Efficient Nucleotide Incorporation and Discrimination in Human DNA Polymerase β*

(Received for publication, March 8, 1996)

William A. Beard‡, Wendy P. Osheroff§, Rajendra Prasad‡, Michael R. Sawaya¶, Madhuri Jaju‡, Thomas G. Wood‡, Joseph Kraut¶, Thomas A. Kunkel§, and Samuel H. Wilson‡‖

From the ‡Sealy Center for Molecular Science, University of Texas Medical Branch, Galveston, Texas 77555-1068, the §Laboratory of Molecular Genetics, NIEHS, Research Triangle Park, North Carolina 27709, and the ¶Department of Chemistry, University of California, San Diego, California 92093-0317

In the crystal structure of a substrate complex, the side chains of residues Asn^{279}, Tyr^{271}, and Arg^{283} of DNA polymerase β are within hydrogen bonding distance to the bases of the incoming deoxynucleoside 5′-triphosphate (dNTP), the terminal primer nucleotide, and the templating nucleotide, respectively (Pelletier, H., Sawaya, M. R., Kumar, A., Wilson, S. H., and Kraut, J. (1994) *Science* 264, 1891–1903). We have altered these side chains through individual site-directed mutagenesis. Each mutant protein was expressed in *Escherichia coli* and was soluble. The mutant enzymes were purified and characterized to probe their role in nucleotide discrimination and catalysis. A reversion assay was developed on a short (5 nucleotide) gapped DNA substrate containing an opal codon to assess the effect of the amino acid substitutions on fidelity. Substitution of the tyrosine at position 271 with phenylalanine or histidine did not influence catalytic efficiency (k_{cat}/K_m) or fidelity. The hydrogen bonding potential between the side chain of Asn^{279} and the incoming nucleotide was removed by replacing this residue with alanine or leucine. Although catalytic efficiency was reduced as much as 17-fold for these mutants, fidelity was not. In contrast, both catalytic efficiency and fidelity decreased dramatically for all mutants of Arg^{283} (Ala > Leu > Lys). The fidelity and catalytic efficiency of the alanine mutant of Arg^{283} decreased 160- and 5000-fold, respectively, relative to wild-type enzyme. Sequence analyses of the mutant DNA resulting from short gap-filling synthesis indicated that the types of base substitution errors produced by the wild-type and R283A mutant were similar and indicated misincorporations resulting in frequent T·dGTP and A·dGTP mispairing. With R283A, a dGMP was incorporated opposite a template thymidine as often as the correct nucleotide. The x-ray crystallographic structure of the alanine mutant of Arg^{283} verified the loss of the mutated side chain. Our results indicate that specific interactions between DNA polymerase β and the template base, but *not* hydrogen bonding to the incoming dNTP or terminal primer nucleotide, are required for both high catalytic efficiency and nucleotide discrimination.

Accurate DNA synthesis during replication and DNA repair is crucial in maintaining genomic integrity. Although DNA polymerases play a central role in these essential processes, the fundamental mechanism by which they select the correct deoxynucleoside 5′-triphosphate (dNTP)[1] from a pool of structurally similar compounds and substrates to accomplish rapid and efficient polymerization is poorly understood. Vertebrate DNA polymerase β (β-pol) has been suggested to play a role in both DNA repair (1–5) and replication (6–8). The x-ray crystal structures of rat and human β-pol in complex with substrates have suggested a detailed model of the chemical mechanism for the nucleotidyl transfer reaction and also have suggested several protein/substrate interactions that may play a role in nucleotide discrimination (9–12). Additionally, these structures allow us to experimentally test model-derived predictions about the role(s) of individual amino acids.

DNA and RNA polymerases, for which the structure has been determined, have been described by analogy to the anatomical features of a hand as consisting of fingers, palm, and thumb subdomains (13). Conserved carboxylates, which bind catalytically essential divalent metal ions, are found in the palm subdomains of these polymerases. The dNTP binding site of β-pol is formed by the DNA template base, the 3′-terminal nucleotide of the primer strand, and the palm and thumb subdomains of the polymerase (10). Only three amino acid residues of the thumb subdomain have side chains that are within hydrogen bonding distance to the nucleotide bases within this binding pocket. These hydrogen bond donors are indiscriminate in that they bond to the O2 of pyrimidines or the N3 of purines in the DNA minor groove (14). The structure of the β-pol ternary complex reveals a single hydrogen bond between the base of the incoming ddCTP and Asn^{279}; Tyr^{271} and Arg^{283} are also within hydrogen bonding distance to the O2 and N3 atoms of the terminal primer and templating base, respectively (Fig. 1). To assess the role of these interactions in nucleotide selection and incorporation, we replaced Tyr^{271}, Asn^{279}, and Arg^{283} with alternate residues by site-directed mutagenesis to remove and/or alter each interaction.

EXPERIMENTAL PROCEDURES

Materials—Poly(dA), p(dT)$_{10}$, and dNTPs were from Pharmacia Biotech Inc. [α-^{32}P]dTTP (3000 Ci/mmol) was from DuPont NEN and T4 DNA ligase was purchased from New England Biolabs.

Mutagenesis of the Human β-Pol Gene—Oligonucleotide site-directed mutagenesis was performed using a procedure described previously (15). M13 phage containing the human β-pol target DNA was propagated using the bacterial host CJ236 (*dut*$^-$*ung*$^-$) and phage DNA purified for use as template. Synthetic oligonucleotide primers containing the desired codon change were annealed to the template DNA and the

* This work was supported in part by National Institutes of Health Grants ES06839, ES06676, and GM52982 and Welch Foundation Grant H-1265 (to S. H. W.), National Institutes of Health Grant GM52860 (to J. K.), National Institutes of Health Grant DK07233 (to M. R. S.), and grants of computer time from the San Diego Supercomputer Center. The costs of publication of this article were defrayed in part by the payment of page charges. This article must therefore be hereby marked "*advertisement*" in accordance with 18 U.S.C. Section 1734 solely to indicate this fact.

‖ To whom correspondence should be addressed.

[1] The abbreviations used are: dNTP, 2′-deoxynucleoside 5′-triphosphate; β-pol, DNA polymerase β; ddTTP, 2′,3′-dideoxythymidine 5′-triphosphate; T·P, template·primer; Cα, α-carbon; MES, 4-morpholineethanesulfonic acid.

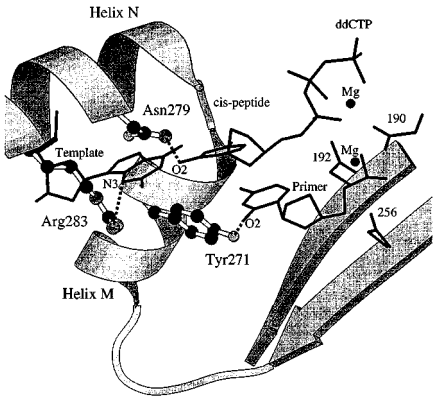

FIG. 1. **Ribbon drawing of the dNTP binding pocket of rat DNA polymerase β.** The side chains of residues Asn^{279}, Tyr^{271}, and Arg^{283} of DNA polymerase β are within hydrogen bonding distance (*dashed lines*) to the bases of the incoming dideoxynucleoside triphosphate (*ddCTP*), the terminal primer nucleotide, and the templating nucleotide, respectively (10). These residues can hydrogen bond indiscriminately to the O2 of pyrimidines or the N3 of purines in the DNA minor groove. They are part of two α-helices, M and N, which are interrupted by a cis-peptide bond between residues Gly^{274}-Ser^{275}. The observed distances from the side chain hydrogen bond donor and O2 or N3 are 2.7, 3.0, and 3.2 Å for Tyr^{271}, Asn^{279}, and Arg^{283}, respectively (10). Also indicated are active site carboxylate side chains (Asp^{190}, Asp^{192}, Asp^{256}) which coordinate two Mg^{2+} ions in the palm subdomain. This figure was made with MOLSCRIPT (30).

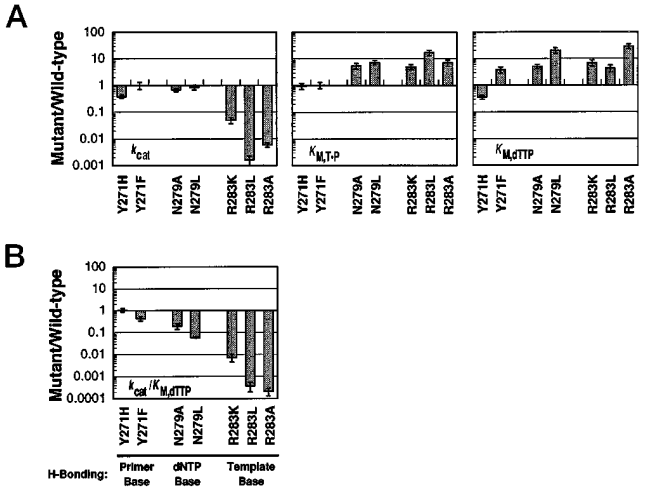

FIG. 2. **Steady-state kinetic parameters for wild-type and mutant β-pol.** Assays were performed as described under "Experimental Procedures." The substrate concentrations were varied from at least 0.3 to 3 × K_m under saturating concentrations of the other (*i.e.* >4 × K_m). Initial velocities were fitted to the Michaelis equation by nonlinear least squares methods. The results represent the mean and S.E. of at least two independent determinations. *A*, the k_{cat}, $K_{m,T\cdot P}$, and $K_{m,dTTP}$ values for the mutant enzymes relative to wild-type are presented in the *left*, *center*, and *right panels*, respectively. The corresponding values for k_{cat}, $K_{m,T\cdot P}$, and $K_{m,dTTP}$ with wild-type enzyme are 0.8 ± 0.1 s^{-1}, 120 ± 30 nM, and 8.6 ± 1.3 μM, respectively. *B*, the catalytic efficiency ($k_{cat}/K_{m,dTTP}$) relative to wild-type enzyme is presented in order of decreasing efficiency. The corresponding value for $k_{cat}/K_{m,dTTP}$ with wild-type enzyme is 8.8 ± 1.6 × 10^4 M^{-1} s^{-1}.

primers extended with Sequenase Version 2.0 (U. S. Biochemical Corp.). The following mutations were introduced into the M13 β-pol vector, 5′ to 3′: Y271F (TAT to TTC), Y271H (TAT to CAC), N279A (AAT to GCG), N279L (AAT to CTG), R283A (AGG to GCG), R283K (AGG to AAA), and R283L (AGG to CTG). To ensure that the resulting β-pol genes contained the desired change, the entire coding sequence of each mutant was confirmed by DNA sequence analysis. The mutated β-pol gene was inserted into the *Cla*I and *Hin*dIII sites of the λP_L promotor-based expression system pWL-11 provided by T. A. Patterson (Ares, Inc.) and overexpressed in *Escherichia coli* TAP56.

Protein Purification—Wild-type and mutant enzymes were purified as described previously (16). All enzyme preparations were assayed for contaminating 3′ → 5′ exonuclease activity on a mismatched primer and had at least 10-fold lower exonuclease activity relative to Klenow fragment (17).

β-Pol Polymerization Assays—Enzyme activities were determined using a standard reaction mixture (50 μl) containing 50 mM Tris-HCl, pH 7.4 (22 °C), 5 mM $MnCl_2$, and 100 mM KCl. Other reaction conditions are described in the figure legends. Reactions were initiated by addition of enzyme, incubated at 22 °C, and stopped by the addition of 20 μl of 0.5 M EDTA, pH 8. Quenched reaction mixtures were spotted onto Whatman DE-81 filter disks and dried. Unincorporated [α-^{32}P]dTTP was removed, and filters were counted as described (18).

Short Gap Fidelity Assay—A gapped DNA substrate was constructed in which the single-stranded gap contains the *lacZ* α-complementation sequence of M13mp2, which has been modified by the introduction of an in frame opal codon (see Fig. 3*A*). The construction of the gapped substrate will be described in detail elsewhere. Polymerase reactions (20 μl) contained: 20 mM Tris-HCl, pH 8.0, 2 mM dithiothreitol, 25 mM NaCl, 10 mM $MgCl_2$, 5% glycerol, 1 mM ATP, 150 ng (32 fmol) of gapped DNA, 500 μM each dATP, dCTP, dGTP, and dTTP, 400 units of T4 DNA ligase and β-pol. An enzyme titration was performed to determine the amount of each β-pol variant required to completely fill the 5-nucleotide gap (see below). Following incubation at 37 °C for 60 min, reactions were stopped by adding EDTA to 37.5 mM and the products separated on an agarose gel. Gel slices containing covalently closed circular product DNAs were isolated. The DNAs were electroeluted from gel slices and concentrated. DNA samples were introduced into competent *E. coli* cells by electroporation and plated on Petri dishes containing the chromogenic indicator 5-bromo-4-chloro-3-indolyl-β-D-galactoside and a lawn of *E. coli* α-complementation host cells (CSH50) as described (19). Molar ratios of enzyme to DNA used in these assays are as follows: 25:1 for wild-type, N279A, N279L; 100:1 for Y271H, Y271F; 200:1 for R283K, R283L; 250:1 for R283A.

Structure Determination—The human wild-type and mutant enzymes were complexed with DNA by mixing 54 μl of enzyme (20 mg/ml in 0.1 MES, pH 6.5, 10 mM $(NH_4)_2SO_4$) with 43 μl template·primer (T·P) (5.5 mg/ml in 20 mM $MgSO_4$) at room temperature. ddTTP was added in 40-fold molar excess to the enzyme-DNA complex. The template and primer sequences are 5′-CAAACTCACAT-3′ and 5′-TGATGTGAG-3′, respectively. Crystals of the complex were grown at room temperature from sitting drops prepared by mixing 5 μl of protein-DNA complex with 5 μl of reservoir containing 13% polyethylene glycol 3350, 180 mM NaCl, 50 mM cacodylate, pH 6.5. Crystals appeared within a week. Macroseeding was employed to enlarge crystal size. Crystals belong to space group $P2_12_12$ (a = 180, b = 57.5, c = 47.9 Å) and are isomorphous with crystals obtained previously (11). The crystals grew to 0.6 × 0.3 × 0.2 mm and diffracted to 3.3 Å. Using a rotating anode x-ray generator equipped with Xuong-Hamlin multiwire area detectors (20), 43,435 observations of 8411 unique reflections were collected with 97% completeness to 3.3 Å.

RESULTS AND DISCUSSION

Expression constructs of human β-pol were prepared: Tyr^{271} was replaced with either histidine or phenylalanine; Asn^{279} was replaced with either alanine or leucine; and Arg^{283} was replaced with either alanine, leucine, or lysine. Each altered human β-pol gene was expressed in *E. coli* and the recombinant enzymes were soluble in the crude cell extracts. Following purification, SDS-PAGE analysis indicated that the mutant β-pol polypeptides had the same apparent molecular weight as the wild-type enzyme and were greater than 99% homogeneous (data not shown).

To compare the catalytic efficiency of the wild-type and mutant enzymes, the steady-state kinetics on a simple T·P system, poly(dA)-p$(dT)_{10}$ with dTTP as the incoming nucleotide, were analyzed (Fig. 2). Whereas the catalytic activity of the Tyr^{271} and Asn^{279} mutants were not significantly influenced (*i.e.* <10-fold), k_{cat} of the lysine, alanine, and leucine mutants of Arg^{283} were decreased greater than 20-, 150-, and 600-fold, respectively (Fig. 2*A*). In contrast, the K_m for T·P was increased with the R283L mutant (17-fold), and the K_m for dTTP was increased to the greatest extent with the R283A mutant (29-fold) (Fig. 2*A*). Catalytic efficiency, as measured by the ratio of k_{cat} and $K_{m,dNTP}$, was not influenced by the histidine substitution at Tyr^{271}, while the phenylalanine mutant displayed a modest

(2-fold) decrease (Fig. 2*B*). Since the phenylalanine substitution had only a small effect on catalytic efficiency, substrate interactions with Tyr^{271} appears to offer very little transition state stabilization. Elimination of the hydrogen bond between the incoming dNTP and the Asn^{279} side chain with an alanine or leucine substitution decreased catalytic efficiency further, but again only modestly (≈10-fold). In this case, catalytic efficiency was dependent solely on the apparent dNTP binding affinity,[2] since k_{cat} of each mutant was similar to wild-type enzyme. The most dramatic decrease in catalytic efficiency was observed for the mutants of Arg^{283} (Ala > Leu > Lys). A 5000-fold decrease in efficiency was observed for the alanine mutant, whereas catalytic efficiency of the lysine mutant, which could potentially hydrogen bond to the template base, was decreased over 100-fold.

In vivo, β-pol is involved in short gap DNA repair (1–3, 5). DNA polymerase β is an ideal polymerase to examine "intrinsic" base substitution fidelity, because it lacks an associated 3′ → 5′ proofreading exonuclease. *In vitro*, pol-β fills these short gaps (≤6 nucleotides) processively, whereas longer gaps are filled distributively (21). The fidelity of β-pol-dependent long gap DNA synthesis (*i.e.* >100 nucleotides) had previously been examined on undamaged (22, 23) and damaged DNA templates (24, 25). To determine the fidelity of wild-type β-pol on a physiologically relevant DNA substrate and to assess the effect of the amino acid substitutions on fidelity, a reversion assay was developed on a short (5 nucleotide) gapped DNA substrate containing an opal codon (Fig. 3*A*). This codon is within the non-essential *lacZα* gene of bacteriophage M13mp2. Polymerase errors that restore α-complementation activity yield a blue or light blue plaque phenotype. This assay can detect eight different base substitution errors.

The result of *in vitro* gap filling synthesis by wild-type β-pol and the mutants described above on the reversion of the opal codon is shown in Fig. 3*B*. Wild-type β-pol produced one revertant per 370 filled gaps (reversion frequency of 27×10^{-4}). Whereas deletion of the hydrogen bond donor at Tyr^{271} did not alter the reversion frequency, alanine substitution at Asn^{279} significantly reduced it signifying an apparent increase in fidelity. This apparent increase in fidelity could reflect a reduced misinsertion rate or a reduced ability to extend mispairs, since both must occur to score a mutant. In contrast, alteration of the Arg^{283} side chain, which interacts with the templating base, dramatically lowered fidelity, as demonstrated by the strong increases in reversion frequency (Fig. 3*B*).

Sequence analyses of the DNA of *lacZα* mutants resulting from short gap filling synthesis indicated that the types of base substitution errors produced by the wild-type and R283A mutant were similar (Table I). However, the frequency of each type of error was much greater for the R283A mutant. The base substitution errors observed in the polymerization products of both enzymes reflected misincorporations resulting in relatively frequent T·dGTP and A·dGTP mispairs. Seven of the eight mispairs detected by this reversion assay were observed in the products of wild-type enzyme and the strong mutator mutant R283A. For the mutant polymerase, a dGMP was incorporated opposite a template thymidine nearly 46% of the time, whereas the correct nucleotide was incorporated only 48% of the time. Additionally, sequence analysis often detected two misincorporations by both wild-type and R283A polymerases within the 5-nucleotide gap. These misincorporations were, in many instances, consecutive, and in one case, three consecutive misincorporations were observed. Consecutive misincorporations had not been observed previously in the forward mutation assay employing a long single-stranded template (22, 23). This suggests that a difference may exist between the fidelity of β-pol during short processive gap filling as compared

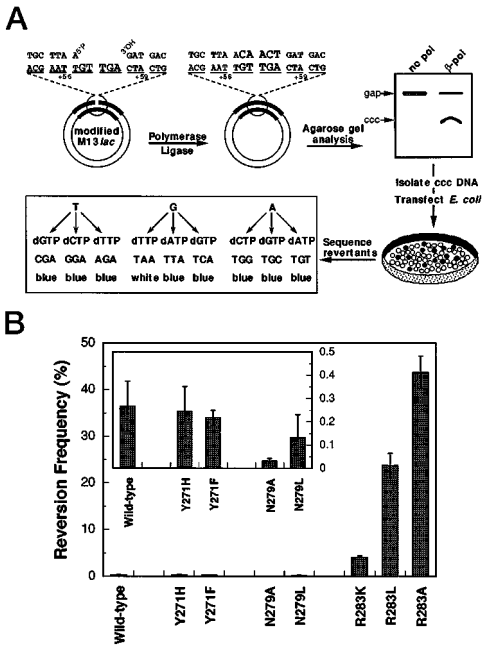

FIG. 3. **Short gap fidelity assay.** *A*, experimental outline for the short gap fidelity assay as described under "Experimental Procedures." *B*, mutation frequencies for the products synthesized by the wild-type and mutant β-polymerases. The background reversion frequency for the assay was ≤0.001%. Frequencies are shown as the mean and standard deviation of at least two independent determinations.

[2] The apparent $K_{m,dNTP}$ determined using a homopolymeric template·primer is equivalent to the equilibrium dissociation constant, K_d, when dissociation of the template·primer does not limit catalytic turnover.

TABLE I
Base substitution specificity of wild-type and R283A β-pol

DNA from 47 wild-type and 92 R283A β-pol revertants was sequenced yielding a total of 49 and 98 base substitution mutations, respectively. Error rates per detectable nucleotide polymerized were calculated as described (19). Multiple base substitution mutations in a revertant were treated as independent events in the calculation.

Template nucleotide	Mismatch (template·dNTP)	Revertant nucleotide	Errors per detectable nucleotide[a]		-Fold increase in errors relative to wild-type
			Wild-type β-Pol revertants[a]	R283A β-Pol revertants[b]	
T	T·dGTP	C	2.9×10^{-3} (32)	460×10^{-3} (61)	160
	T·dCTP	G	0.2×10^{-3} (2)	30×10^{-3} (4)	150
	T·dTTP	A	$\leq 0.1 \times 10^{-3}$ (0)	30×10^{-3} (4)	≥300
G	G·dATP	T	0.2×10^{-3} (2)	15×10^{-3} (2)	75
	G·dGTP	C	0.2×10^{-3} (2)	$\leq 7 \times 10^{-3}$ (0)	≤35
A	A·dCTP	G	0.3×10^{-3} (3)	60×10^{-3} (8)	200
	A·dGTP	C	0.6×10^{-3} (7)	110×10^{-3} (15)	180
	A·dATP	T	0.1×10^{-3} (1)	30×10^{-3} (4)	300

[a] The mutant fraction for wild-type and R283A β-pol DNA synthesis reactions was 27×10^{-4} and 4400×10^{-4}, respectively.
[b] Numbers in parentheses indicate number of base substitution errors observed.

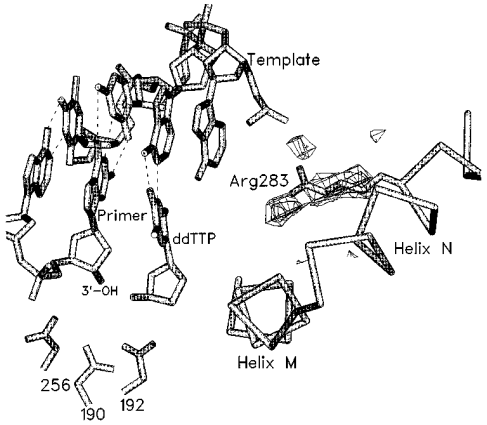

FIG. 4. **Structural comparison of wild-type and alanine mutant of Arg^{283} of human β-pol complexed with DNA and ddTTP.** The structure of the ternary substrate complex of the wild-type and R283A mutant were determined as described under "Experimental Procedures." A $F_{o(R283A)} - F_{o(native)}$ difference Fourier map reveals a negative peak enveloping the Arg^{283} side chain consistent with mutation to alanine. No other significant changes were detected in the structure. The DNA, helices M and N (Arg^{283}), and active site carboxylates (Asp^{190}, Asp^{192}, Asp^{256}) of the wild-type enzyme are superimposed on the difference map. Although the thymidine moiety of ddTTP is observed, the 5′-triphosphate is disordered. In contrast to the rat β-pol ternary complex where the thumb subdomain is in a closed conformation (Fig. 1) (10), the human enzyme (wild-type and mutant) crystallized with the thumb in the open conformation. Therefore, Ala^{283} is moved over 12 Å away from where it is observed in the closed ternary complex.

with distributive DNA synthesis on large gaps. Processive short gap filling synthesis is modulated by the binding of the amino-terminal 8-kDa domain to the downstream 5′-phosphate group in gapped DNA (26).

To understand the structural basis for the lower catalytic efficiency and fidelity of the alanine mutant of Arg^{283}, we determined the x-ray crystal structure of this mutant in complex with substrates (Fig. 4). In contrast to the rat β-pol ternary complex, where the thumb subdomain is in a closed conformation (10), the human mutant β-pol ternary complex crystallized in a different crystal packing form with the thumb in the open conformation (space group $P2_12_12$). Hence, Ala^{283} is moved over 12 Å away from the template. This open conformer had been observed previously when the wild-type human enzyme is bound to the blunt end of duplex DNA (11). We have been unable to crystallize the mutant with the thumb in the closed conformation. There is electron density corresponding to the incoming thymidine moiety of ddTTP at the primer 3′ terminus; however, the ddTTP had not reacted with the primer and the 5′-triphosphate is disordered and not visible. A $F_{o(R283A)} - F_{o(native)}$ difference Fourier map reveals a negative peak enveloping the Arg^{283} side chain consistent with mutation to alanine (Fig. 4). No other significant changes were detected between wild-type and mutant enzymes. Superimposition of the palm subdomains of the rat ternary closed complex (space group $P6_1$) with the mutant, or wild-type, open ternary complex reveals that the N3 position of the templating adenine in the open complex is 3.1 Å from where it is observed in the closed complex. Superimposition of 97 Cαs from the palm subdomains of the rat ternary closed complex (PDB file 2bpf, see Ref. 10) and the ternary open complex of wild-type or R283A human β-pol gave a root mean square deviation of 0.75 Å. The terminal primer sugars in the open and closed complexes are very near one another, $\Delta C3' = 0.8$ Å, whereas the equivalent sugar positions for the templating base and incoming dNTP are displaced 3.8 and 1.2 Å, respectively. Since dNTPs can bind to the enzyme in the open conformation (12), closing of the thumb not only positions the dNTP but positions the templating base for efficient nucleotide incorporation.

The fingers and thumb subdomains are structurally diverse among the different classes of polymerases, and except for β-pol, the dNTP binding site is not clearly defined. Therefore, the functional role of each subdomain may be unique to each class of polymerase, and care must be taken in extrapolating the present results to the thumb subdomain of other DNA polymerases (27).

In summary, fidelity assays coupled with kinetic and structural evaluation of the alanine mutant of Arg^{283} indicate that this residue plays a central role in nucleotide discrimination by correctly positioning and stabilizing the templating base for efficient nucleotide incorporation. Although the guanidinium group of Arg^{283} is within hydrogen bonding distance to N3 of the template guanine, the hydrogen bond geometry is unfavorable. Therefore, correct van der Waal's interactions may also be important at this site. This is consistent with the low catalytic efficiency and reduced fidelity exhibited by the lysine mutant of Arg^{283}, which would be expected to preserve hydrogen bonding to the templating base. Our results support the hypothesis that discrimination and catalytic efficiency are modulated by polymerase interactions near the templating base and are sensitive to precise Watson-Crick base pairing by possibly "sensing" C1′ distances and bond angle geometry (28, 29). In contrast, alteration of direct interactions with the incoming dNTP decreased dNTP binding affinity but not fidelity. Thus, the coupling between catalytic efficiency and discrimination is residue-specific. Our results indicate that we can modulate discrimination and catalytic efficiency based upon ternary complex crystal structures, and site-directed mutagenesis will be a productive avenue for future analysis of polymerase structure-function relationships.

Acknowledgments—We thank Dinh Nguyen and Alan Clark for the sequencing of β-pol revertants; T. A. Patterson for the pWL-11 expression vector; and R. S. Lloyd, S. Mitra, S. Prakash, and B. Van Houten for critical reading of the manuscript.

REFERENCES

1. Wiebauer, K., and Jiricny, J. (1990) *Proc. Natl. Acad. Sci. U. S. A.* **87,** 5842–5845
2. Dianov, G., and Lindahl, T. (1994) *Curr. Biol.* **4,** 1069–1076
3. Horton, J. K., Srivastava, D. K., Zmudzka, B. Z., and Wilson, S. H. (1995) *Nucleic Acids Res.* **23,** 3810–3815
4. Singhal, R. K., Prasad, R., and Wilson, S. H. (1995) *J. Biol. Chem.* **270,** 949–957
5. Sobol, R. W., Horton, J. K., Kühn, R., Gu, H., Singhal, R. K., Prasad, R., Rajewsky, K., and Wilson, S. H. (1996) *Nature* **379,** 183–186
6. Linn, S. (1991) *Cell* **66,** 185–187
7. Jenkins, T. M., Saxena, J. K., Kumar, A., Wilson, S. H., and Ackerman, E. J. (1992) *Science* **258,** 475–478
8. Sweasy, J. B., and Loeb, L. A. (1992) *J. Biol. Chem.* **267,** 1407–1410
9. Sawaya, M. R., Pelletier, H., Kumar, A., Wilson, S. H., and Kraut, J. (1994) *Science* **264,** 1930–1935
10. Pelletier, H., Sawaya, M. R., Kumar, A., Wilson, S. H., and Kraut, J. (1994) *Science* **264,** 1891–1903
11. Pelletier, H., Sawaya, M. R., Wolfle, W., Wilson, S. H., and Kraut, J. (1996) *Biochemistry*, in press
12. Pelletier, H., Sawaya, M. R., Wolfle, W., Wilson, S. H., and Kraut, J. (1996) *Biochemistry*, in press
13. Kohlstaedt, L. A., Wang, J., Friedman, J. M., Rice, P. A., and Steitz, T. A. (1992) *Science* **256,** 1783–1790
14. Seeman, N. C., Rosenberg, J. M., and Rich, A. (1976) *Proc. Natl. Acad. Sci. U. S. A.* **73,** 804–808
15. Kunkel, T. A., Roberts, J. D., and Zakour, R. A. (1987) *Methods Enzymol.* **154,** 367–382
16. Beard, W. A., and Wilson, S. H. (1995) *Methods Enzymol.* **262,** 98–107
17. Roberts, J. D., Bebenek, K., and Kunkel, T. A. (1988) *Science* **242,** 1171–1173
18. Beard, W. A., and Wilson, S. H. (1993) *Biochemistry* **32,** 9745–9753
19. Bebenek, K., and Kunkel, T. A. (1995) *Methods Enzymol.* **262,** 217–232
20. Hamlin, R. (1985) *Methods Enzymol.* **114,** 416–452
21. Singhal, R. K., and Wilson, S. H. (1993) *J. Biol. Chem.* **268,** 15906–15911
22. Kunkel, T. A. (1985) *J. Biol. Chem.* **260,** 5787–5796
23. Kunkel, T. A., and Soni, A. (1988) *J. Biol. Chem.* **263,** 14784–14789
24. Feig, D. I., and Loeb, L. A. (1993) *Biochemistry* **32,** 4466–4473
25. Feig, D. I., and Loeb, L. A. (1994) *J. Mol. Biol.* **235,** 33–41
26. Prasad, R., Beard, W. A., and Wilson, S. H. (1994) *J. Biol. Chem.* **269,** 18096–18101
27. Joyce, C. M., and Steitz, T. A. (1995) *J. Bacteriol.* **177,** 6321–6329
28. Kennard, O. (1988) in *Structure and Expression, DNA and Its Drug Complexes* (Sarma, R. H., and Sarma, M. H., eds) Vol. 2, pp. 1–25, Adenine Press, Guilderland, NY
29. Echols, H., and Goodman, M. F. (1991) *Annu. Rev. Biochem.* **60,** 477–511
30. Kraulis, P. J. (1991) *J. Appl. Crystallogr.* **24,** 946–950